Journal of Electrical and Computer Engineering Innovations
(JECEI)
Journal homepage: http://www.jecei.sru.ac.ir

SRTTU

JECEI

Research paper

Using Convolutional Sparse Representation and Discrete Wavelet Decomposition for Satellite Image Pan-sharpening

A. Sharifi*

Department of Surveying Engineering, Faculty of Civil Engineering, Shahid Rajaee Teacher Training University, Tehran, Iran.

Article Info

Article History:
Received 18 November 2018
Reviewed 15 January 2019
Revised 9 March 2019
Accepted 11 May 2019

Keywords:
Remote Sensing
Image fusion
Pan-sharpening
Discrete wavelet transform
Convolutional sparse representation

*Corresponding Author's Email Address:
a_sharifi@sru.ac.ir

Abstract

Background and Objectives: High resolution multi-spectral (HRMS) images are essential for most of the practical remote sensing applications. Pan-sharpening is an effective mechanism to produce HRMS image by integrating the significant structural details of panchromatic (PAN) image and rich spectral features of multi-spectral (MS) images.
Methods: The traditional pan-sharpening methods incur disadvantages like spectral distortion, spatial artifacts and lack of details preservation in the fused image. The pan-sharpening approach proposed in this paper is based on integrating wavelet decomposition and convolutional sparse representation (CSR). The wavelet decomposition is performed on PAN and MS images to obtain low-frequency and high-frequency bands. The low-frequency bands are fused by exploring the CSR based activity level measurement.
Results: The HRMS image is restored by implementing the inverse transform on fused bands. The fusion rules are constructed, thus to transfer the crucial details from source images to the fused image effectively.
Conclusion: The proposed method produces HRMS images with rational spatial and spectral qualities. The visual outcomes and quantitative measures approve the eminence of the proposed fusion framework.

Introduction

Due to technological constraints and physical limitations, the remote sensing sensors produce the images with a striking trade-off between spatial and spectral resolutions. Most of the high-resolution optical sensors such as IKONOS, Pleiades, and WorldView-3 usually produce a panchromatic (PAN) image with low spectral resolution/high spatial resolution and a multi-spectral (MS) image composed of several bands, with low spatial resolution/high spectral resolution [1]. The MS and PAN images are acquired simultaneously over the same geographical terrain i.e., the two images represent the same scene.

The High-resolution MS (HRMS) images with superior resolution features in both spatial and spectral domains are most desirable in applications like hazard monitoring, land-cover and land-use classification, and environmental change detection [2]. Pan-sharpening (PS) is a significant section of multi sensor data fusion, aims to generate a HRMS image that is more suitable for human and machine perception than the individual input images. The objective of a PS mechanism is to produce a HRMS image, inheriting the spatial quality of the PAN image and maintaining the spectral richness of the MS image. Let X_k, $k = 1, 2, \ldots, N$ be the MS image with N number of bands and Y be the PAN image. The MS image upsampled to the size of the PAN image is denoted as $\tilde{X}_k$ and $\hat{X}_k$ represents the estimated HRMS image. The pansharpened image is obtained by adding a spatial detail image, D, to the up-sampled image, $\tilde{X}_k$, as below.

$$\hat{X}_k = \tilde{X}_k + g_k.D, \quad k = 1,2, \dots, N \tag{1}$$

The dimension of D is the same as that of up-sampled MS and pansharpened images. However, the CS and MRA methods mainly differ in the synthesis process by which the spatial detail image, D is estimated. The spatial detail image, D is crucial in deciding the quality of the fused image. In Eq.(1), $g_k = [g_1, g_2, \dots, g_N]$ is a vector of injection gains, which are band-specific. For CS based methods, the detail image is expressed as,

$$D = Y - \sum_{k=1}^{N} w_k.\tilde{X}_k \tag{2}$$

The selection of parameters like injection gains (g_k) and the weight vector (ω_k) are determined by the specific CS algorithm. The weight vector, ω_k specifies the proportion in which each band has to be preferred for the weighted sum of MS bands. The difference between the PAN image and the weighted sum of MS bands is proportional to spectral distortion in the fused image. The familiar CS based methods are intensity-hue-saturation (IHS) [3], principal component analysis (PCA) [4] and Gram-Schmidt transform (GS) [5]. As a modification to existing CS based methods, a novel gradient transferring method is proposed which significantly reduces the spectral distortion [6].

For MRA based methods, the spatial detail image is constructed as:

$$D = Y - Y_L \tag{3}$$

where, the variant Y_L contains the low-pass details of the PAN image Y. The particular MRA algorithm determines the type of the filter used to determine Y_L and the injection gain vector g_k. The reputable MRA methods are based on wavelets [7], atrous wavelet transform (ATWT) [8], additive wavelet luminance proportional (AWLP) [9], fourier transform weighted red-black wavelets [10], modulation transfer function-generalized lapalician pyramid (MTF-GLP) [11]. The CS methods preserve the requisite spatial details; however, they induce distortion in spectral information of the final outcome. The first sparse representation (SR) based pan-sharpening method was proposed by Li and Yang [12], and the problem of PS is treated as a restoration process. In this method, the fused images patches are assumed to be sparse over a dictionary that is constructed by extracting random patches from HRMS images. To achieve adequate fusion quality, the required size and process of the dictionary construction lead to extensive computational cost. Furthermore, the HRMS image patches may not be available. The pan-sharpening methods can be grouped into two categories: (i) The dictionary constructed by the patches extracted from both the PAN and MS images [13]. (ii) The dictionary constructed by the patches of low resolution image [14]. Unlike the aforementioned PS methods, dictionaries constructed from low and high frequency components of MS image by random sampling is proposed in [15]. In this research, a three steps SR-based pansharpening method was proposed. In the first step, they constructed the high frequency and low frequency dictionaries with the spectral information of MS images so that the reconstructed MS image could achieve the best fidelity effect or decrease the spectral distortion of the sharpening result. Then, PAN image was decomposed into high-frequency component (HFC) and low-frequency component (LFC) by the high frequency (HF) and low frequency dictionaries. Hence, the HFC of PAN image could fit the spatial detail and spectral features of MS image. Finally, the MS image and the HFC of PAN image have been merged to reconstruct the MS image. Moreover, a single dictionary learned from HRMS images is exploited for SR based pan-sharpening [16]. The pan-sharpening paradigms based on multi-scale decomposition combined with the SR are effective in terms of spatial and spectral quality trade-off and computational complexity [17]. To reduce the spatial and spectral distortions effectively, the PS paradigm is formulated based on particle swarm optimization combined with the signal decomposition [18]. The sparse representation based methods are likely to yield improved performance over the conventional and model-based PS methods. However, the SR based pan-sharpening methods usually follow a patch-partition based approach, and the processing of patches on an individual basis overlooks the consistency constraint. While reconstructing images the averaging mechanism is deployed on overlapped patches, which results in loss of spatial structure of the image. Sparse representation performed on overlapped patches results in multi-valued representation (because of the processing of overlapped patches, the representation yields different values for a specific feature present in the original image), which is not optimal over the entire image. To address these issues in existing pan-sharpening methods, a newly developed signal decomposition scheme, known as convolutional sparse representation (CSR) is adapted. CSR mechanism models the entire image rather than repeatedly considering individual patches, which enables preservance of spatial structure and lead to a single-valued representation [19]. The CSR based fusion rule is applied to the bands in the transform domain rather in the imaging domain. The fusion rules implemented are pertinent to the wavelet coefficients.

To overcome the problems of traditional PS approaches, this paper presents an efficient pan-sharpening (PS) method by taking the complementary advantages of multi-scale decomposition, particularly the discrete wavelet transforms (DWT) and CSR [20]. In the proposed method, the source images are decomposed into low and high-frequency bands using wavelet transform. The shift-invariance feature can be attained by exploring the CSR, which is crucial for image fusion. The conventional 'max-absolute' and 'direct averaging' fusion rules result in low-contrast regions in the fused image. The high-frequency bands are fused based on the relative wavelet energy estimated over a specified region. The experimental results validate that the fusion rules exploited in the proposed work successfully transfer the pertinent features from source images to the fused image. Section 2 details the proposed pan-sharpening approach. The experiments result and detailed analysis are given in Section 3. Section 4 concludes the paper.

Proposed method

This section illustrates the proposed pan-sharpening scheme using the integration of wavelet transform and convolutional sparse representation. The low-resolution MS (LRMS) image, X is interpolated to the size of PAN image and represented as $\tilde{X}_k$. The first two moments of PAN image, Y, and the up-sampled LRMS image, $\tilde{X}_k$, are used to produce corresponding pan image Y_k. For each band, i.e., *k=1, 2 .... N.*; the proposed pan-sharpening framework is described in Fig. 1. To overcome the customary disadvantages in pan-sharpening methods, the CSR is adapted into fusion rules in the transform domain.

A. Convolutional sparse representation

Sparse representation is a widely used technique for a very broad range of signal and image processing applications. Given a signal s and a dictionary matrix D, sparse coding is the inverse problem of finding the sparse representation x with only a few non-zero entries such that $Dx \approx s$. Most sparse coding algorithms optimize a functional consisting of a data fidelity term and a sparsity inducing penalty:

$$arg\min_x \frac{1}{2}\|Dx - s\|_2^2 + \lambda R(x) \quad (4)$$

where $R(x)$ denotes a sparsity inducing function.

If the dictionary D is analytically defined and corresponds to a linear operator with a fast transform (e.g. the Discrete Wavelet Transform), a representation for an entire signal or image can easily be computed. More recently, however, it has been realised that improved performance can be obtained by learning the dictionary from a set of training data relevant to a specific problem; this inverse problem is known as dictionary learning. In this case computing a sparse representation for an entire signal is not feasible, the usual approach being to apply the decomposition independently to a set of overlapping blocks covering the signal [21].

The convolutional form of representation originated as a hypothesis of modifying the convolutional neural networks by [22]. The convolutional sparse representation is treated as an alternative representation of SR, produce a convolutional decomposition of an entire image subjected to a sparsity constraint. The main objective of CSR is to model an image as a sum over a set of convolutions of unknown coefficient maps $\{x_m\}$, with their corresponding dictionary filters $\{d_m\}$. By regularizing x_m with sparsity prior, the entire image S is modeled using CSR as:

$$arg\min_{\{x_m\}} \frac{1}{2}\|d_m * x_m - S\|_2^2 + \lambda \textstyle\sum_m \|x_m\|_1, \; m = 1, \dots, M. \quad (5)$$

where, λ is a regularization parameter (a scalar) that controls balance between sparsity and reconstruction error, while the symbol *'*'* represents convolution operation. M denotes the number of dictionary filters. The dictionary filters are learned using finite number of training images as

$$arg\min_{\{d_m\}\{x_m\}} \frac{1}{2}\|d_m * x_m - s_k\|_2^2 + \lambda \textstyle\sum_m \|x_m\|_1 s.t \|d_m\|_2 = 1. \quad (6)$$

where, s_k denote the training images used to learn dictionary filters.

The learned dictionary filters yield less redundancy and the coefficient maps, x_m, preserves the essential spatial structures in the fused images. The CSR model is given in Eq. (6) can be regarded as a convolutional form of well-known basis pursuit problem and termed as CBPDN (convolutional basis pursuit denoising) [23].

The CSR model is designed to analyze the shift-invariant sparse representation, which remains an essential property in image fusion. The redundancy generated by the overlapped pixels as in the case of SR based schemes can be eliminated with CSR by learning the dictionary filters from the whole image. These underlying features preserve the spatial structure in the fused image. In sparse representation scheme, the sparse coefficient vector, α for each of the image patch is estimated using an over-complete dictionary, D, as

$$\alpha = argmin\|a\|_1 \; subject\ to \; \|s - D_\alpha\|_2^2 \le \epsilon \quad (7)$$

Here, ϵ is the admissible error.

The entire image, S, can be expressed as a dot product of dictionary D, and the sparse coefficient vectors, α corresponding to the image patches. i.e $S = \sum_j D_j \alpha_j, j = 1,2, \dots, J$. With J number of patches extracted from the image S, s and α are the patch and coeffcients matrices respectively.

In CSR, the image S can be expressed as convolutions of dictionary elements, d_m and each feature maps, x_m. i.e., $S=\sum_m d_m * x_m$. The size and number of the dictionary filters can be chosen arbitrarily. The size of the coeffcients maps, x_m are same as the image S, and the index, m is same as that of the dictionary filters, d_m.

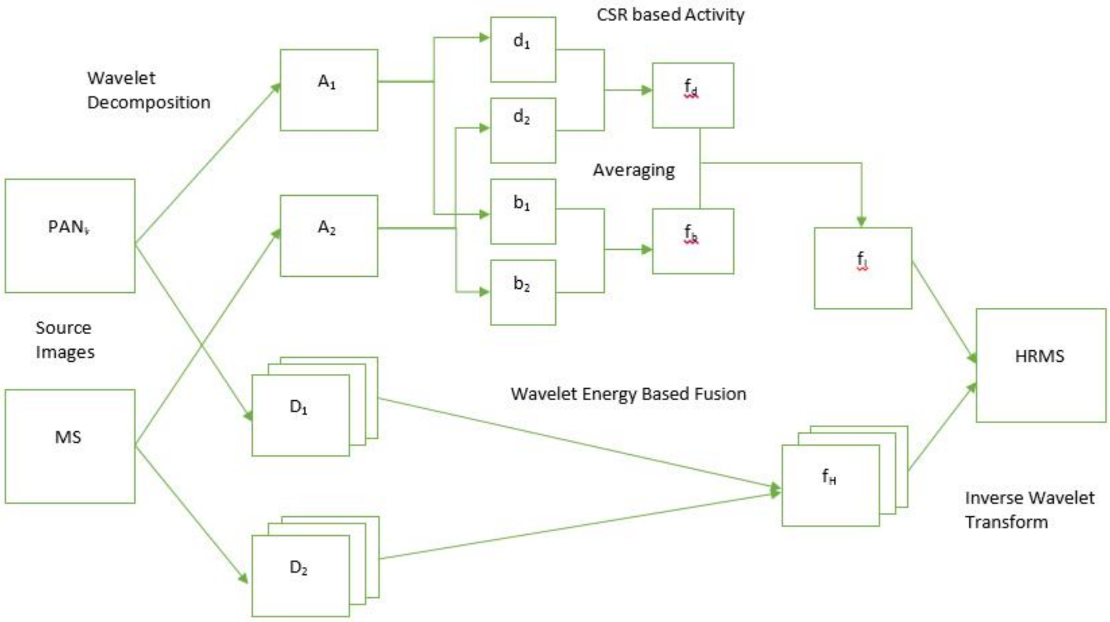

Fig. 1: The Proposed Pan-sharpening Schematic. A_1,A_2 : Low-Frequency bands; D_1,D_2 : High-Frequency bands; d_1,d_2: detail layers; b_1,b_2: base layers; f_d: fused detail layer; f_b: fused base layer; f_L: fused Low-Frequency band; f_H: fused High-Frequency band.

B. Decomposition using wavelet transform

The level of decomposition is an important factor that affects fusion performance. If the decomposition level is high, a single coefficient in the transform domain influences relatively a large area of the image. Hence, a small error in decomposed bands causes severe artifacts in the resultant image obtained by the inverse transformation. The source images, $\tilde{X}_k$ and $\tilde{Y}_k$ are decomposed using wavelet transform to generate the corresponding low-frequency bands $\{A_{\tilde{X}_k}, A_{Y_k}\}$ and high-frequency bands $\{D_{\tilde{X}_k}, D_{Y_k}\}$.

At a given scale J, a finite number of translations are used in applying multi-resolution analysis to obtain a finite number of scaling and wavelet coefficients. The signal can be represented in terms of these coefficients as below.

$$f(x)=\sum_k c_{Jk}\phi_{Jk}(x)+\sum_{j=1}^{J}\sum_k d_{jk}\psi_{jk}(x) \quad (8)$$

where c_{Jk} are the scaling coefficients, d_{jk} are the wavelet coefficients, $\phi(x)$ is low pass filter function, and $\psi(x)$ is high pass filter. The first term in Eq. (8) gives the low-resolution approximation of the signal while the second term gives the detailed information at resolutions from the original down to the current resolution J. At each level of decomposition, the signal is split into high frequency and low frequency components; the low frequency components can be further decomposed until the desired resolution is reached. When multiple levels of decomposition are applied, the process is referred to as multi-resolution decomposition. In practice when wavelet decomposition is used for image fusion, one level of decomposition can be sufficient, but this depends on the ratio of the spatial resolutions of the images being fused [24].

Fusion of low-frequency bands CSR is an efficient sparse coding paradigm to represent the entire image rather than using the local patch processing strategy as below.

$$arg\min_{\{s_i\}}\frac{1}{2}\left\|\sum_i z_i * s_i - I\right\|_2^2+\lambda\sum_i\|s_i\|_1 \quad (9)$$

where, λ is a regularization parameter, z_i is dictionary filters, s_i is the unknown sparse coefficient maps, and '$*$' represents convolution operator.

Various image fusion methods have been adapted a composition, separating a source image into base and detail layers [25]. The approximate bands are further decomposed into its constituent base and detail layers. The solution of the following optimization problem yields the base layer, $A_{\tilde{X}_k}^b$, of low-pass band $\{A_{\tilde{X}_k}\}$,

$$arg\min_{A_{\tilde{X}_k}^b}\left\|A_{\tilde{X}_k}-A_{\tilde{X}_k}^b\right\|_F^2+\eta\left(\left\|g_x+A_{\tilde{X}_k}^b\right\|_F^2+\left\|g_y+A_{\tilde{X}_k}^b\right\|_F^2\right) \quad (10)$$

The parameters $g_x = [-1\ 1]$ and $g_y = [-1\ 1]^T$ are horizontal and vertical gradient operators, respectively. The notion $\|.\|_F$ represents Frobenius norm. The regularization parameter η is selected as 5 for the proposed CSR based pan-sharpening scheme. Once, the base layer is determined by solving the Tikhonov regularization (Eq.(10)) using fast Fourier transform, the detail layer can be estimated as

$$A^d_{\tilde{X}_k} = A_{\tilde{X}_k} - A^b_{\tilde{X}_k} \tag{11}$$

A set of dictionary filters $Z_m, m = 0,1,\dots,M.$ are learned from the low-frequency bands by using the dictionary learning algorithm.

The sparse coefficient maps $S_{i,m}$ for each of the detail layer $A^d = \left\{A^d_{\tilde{X}_k}, A^d_{Y_k}\right\}$ are obtained by solving the CSR model.

C. Fusion of high-frequency bands

The fusion of high frequency bands depends on the ingredient wavelet energy, and is defined as

$$E(w) = \frac{\sum_{p=1}^{P}\sum_{q=1}^{Q} G(p,q)^2}{P \times Q} \tag{12}$$

where, *G(p,q)* is the wavelet coefficient at the spatial location *(p,q)* and *w* is a local window of size *P × Q*. The fused high frequency band, D_f is produced by imposing the following rule.

$$D_{fk}(p,q) = \begin{cases} D_{\tilde{X}_k}(p,q)\, if\ E\left(w_{\tilde{X}_k}(p,q)\right) > E\left(w_{Y_k}(p,q)\right) \\ D_{Y_k}(p,q)\ , otherwise \end{cases} \tag{13}$$

where, $w_{\tilde{X}_k}(p,q)$ and $w_{Y_k}(p,q)$ are the windows centered at the pixel locations *(p,q)* of the bands $D_{\tilde{X}_k}$ and D_{Y_k} , respectively.

Finally, the k^{th} band of HRMS image $\hat{X}_k$ is reconstructed by performing the inverse wavelet transform on the fused components A_{fk} and D_{fk}.

Simulation and results

In this section, the proposed pan-sharpening method is validated with datasets from two satellite images including Pleiades and IKONOS which were acquired from Tehran (17 June 2010) and Kermanshah (11 November 2017), respectively. The proposed method is compared with four state-of-the art methods: FIHS from CS category, MTF-GLP from MRA category, SR-CD from sparse representation, and SR-WT from multi-scale decomposition based methods. Four quantitative measures including correlation coefficient (CC), root mean square error (RMSE), spectral angle mapper (SAM), and universal image quality index (UIQI) are used to validate the efficacy of the proposed method. The execution mechanism for FIHS, SR-CD, and MTF-GLP methods are available online developed by [26]. For the implementation of the proposed method, DWT with two level decomposition is used for the decomposition of source images. The particle swarm optimization (PSO) method was used for optimization process. Since all evolutionary-based optimization methods are based on a random process, the PSO results varied with different trials. As the PSO is a fast optimization method, it converged after 34 iterations, while the number of particles reached 100. After ten trials, the regularization parameter λ in CSR (Eq. (7)) is selected as 0.15 to maintain a balance between the computational effort and performance outcomes and the local window size to measure the wavelet energy is set as 5×5. All the experiments are conducted with MATLAB2013b, on a personal computer with CPU intel core i3 @ 3.10 GHz, 4 GB RAM.

A. Experiments with Pleiades dataset

Pleiades sensor produce a 0.5-m PAN image and a 2-m MS image having four bands. The source images are filtered with 3×3 Gaussian filter and down-sampled by a factor four. Image size is 400*400 pixels, data quantization is 12 bit per pixel, and SNR for PAN and MS bands are 147 and 130, respectively. The source images and visual outcomes of eight different methods along with the proposed method's outcome are presented in Fig. 2. The corresponding quantitative measures are detailed in Table 1.

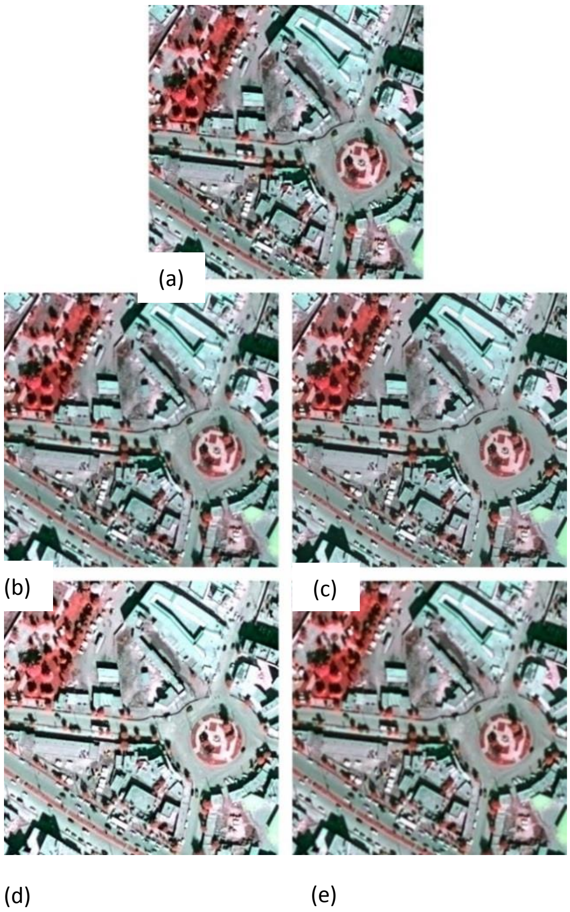

(a) (b) (c) (d) (e)

Fig. 2: Visual results of Pleiades data for (a) Proposed method, (b) FIHS, (c) MTF-GLP, (d) SR-CD, (e) SR-WT.

It can be seen in Fig. 2 that, the outcomes of FIHS, and SR-CD are exhibiting spectral distortion and appears to be blurred compared with the reference image. The wavelet-based method, SR-WT suffers from minimal blocking artifacts particularly at the roofs of the buildings. The results of MTF-GLP, appears to have better visual quality. The outcome of the proposed method is relatively in a close match with the reference.

Table 1: Accuracy assessment of pan-sharpening algorithms using correlation coefficient (CC), root mean square error (RMSE), spectral angle mapper (SAM), and universal image quality index (UIQI) and consumption time for Pleiades and IKONOS dataset

Dataset	**Pleiades**					**IKONOS**				
Method	**CC**	**RMSE**	**SAM**	**UIQI**	**Time (s)**	**CC**	**RMSE**	**SAM**	**UIQI**	**Time (s)**
FIHS	0.738	14.511	2.816	0.722	6.17	0.780	13.231	3.136	0.751	4.59
MTF-GLP	0.768	13.912	2.717	0.741	7.35	0.814	12.832	2.505	0.794	5.68
SR-CD	0.804	12.257	2.390	0.790	8.16	0.825	11.577	2.322	0.814	6.73
SR-WT	0.791	14.180	2.563	0.757	4.78	0.821	12.419	2.474	0.793	3.04
Proposed	0.804	11.555	2.323	0.793	4.31	0.828	11.503	2.355	0.825	2.37

It is obvious from the zoomed portions that, the proposed method better preserves the spatial structures and yields the minimum possible spectral distortion. From the quantitative measures presented in Table 1, it is evident that the proposed method is effective in maintaining the reasonable balance between the spatial and spectral features in the pansharpened image.

B. Experiments with IKONOS datasets

The source images are 1-m PAN image and 4-m MS image with four bands, captured by the IKONOS sensor. The pan-sharpening process is executed on the original data set further, for comparison purpose the fused outcome is down-sampled to the size of the original MS image. The size of image is 200*200 pixels, data quantization is 11 bit per pixel, and SNR for both PAN and MS bands is 45. The visual outcomes of different methods used for comparison are shown in Fig. 3.

The outcome of the FIHS method suffers from intensity distortion. The fusion outcome of SR-WT and MTF-GLP methods are unable to effectively preserve the spectral details. It is difficult to analyze the performance of SR-CD and the proposed method visually. The quantitative measures and the computation times for each method used to fuse the original images are presented in Table 1. The proposed method uses about 3-5 s to generate a fused image in two dataset, which the time costs are acceptable related to other methods.

The proposed method yields optimal values for CC, RMSE, UIQI and second-best value for SAM. It is evident from the three sets of results for IKONOS data, SR-CD and the proposed method outcomes exhibit relatively better performance. The comprehensive experimental results obtained from reduced scale and full-scale validation approved that the proposed framework effectively overcome the drawbacks of conventional SR-CD method. The proposed method yields 1.993% improvement compared with the second-best results in spectral distortion index (SAM) for Pleiades dataset. Also the proposed method accomplishes optimal values for the overall quality measures CC and RMSE. The visual and quantitative results confirmed that the proposed method effectively preserves all the requisite details in the fused image.

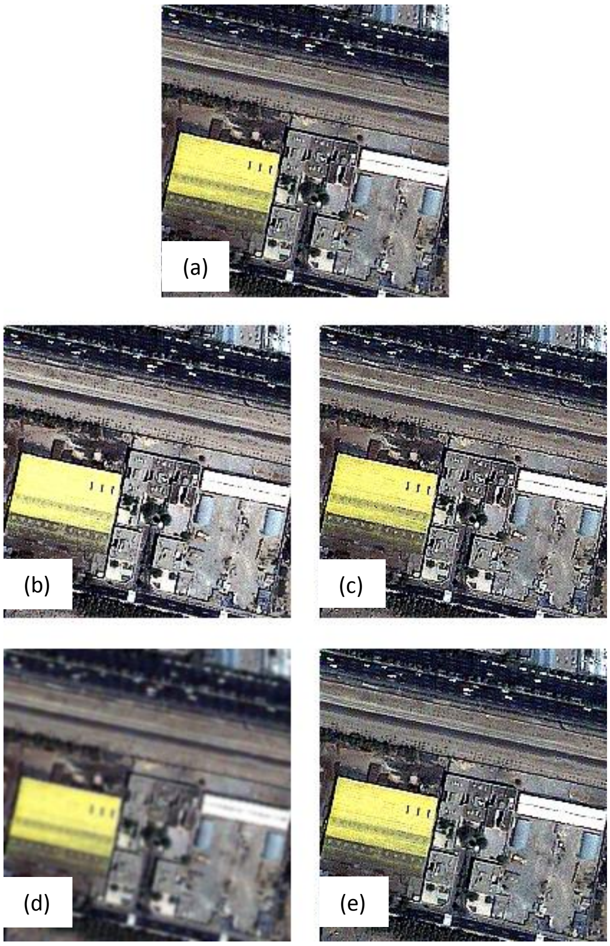

Fig. 3: Visual results of IKONOS data for Visual results of Pleiades data for (a) Proposed method, (b) FIHS, (c) MTF-GLP, (d) SR-CD, (e) SR-WT.

It can be seen in Fig. 3 that, the outcomes of FIHS, and SR-CD are exhibiting spectral distortion and appears to be blurred compared with the reference image. The wavelet-based method, SR-WT suffers from minimal blocking artifacts particularly at the roofs of the buildings. The results of MTF-GLP, appears to have better visual quality. The outcome of the proposed method is relatively in a close match with the reference MS image. It is obvious from the zoomed portions that, the proposed method better preserves the spatial structures and yields the minimum possible spectral distortion.

Conclusion

This paper presents an effective remote sensing image fusion mechanism based on wavelet decomposition and convolutional sparse representation. CSR is a recently developed model as an alternative to SR that can overcome the drawbacks of traditional patch processing strategy used in sparse representation methods. CSR based fusion mechanism yields a single valued and shift-invariant output. The source images are decomposed into corresponding low-frequency and high-frequency bands. CSR paradigm is adapted to fuse the low-frequency bands. The wavelet energy evaluated over a local window region is employed to fuse the high-frequency bands.

Finally, the inverse wavelet transform applied over fused low and high-frequency bands results in the requisite high-resolution MS (HRMS) image. To validate the proposed method, experiments are conducted on degraded data and original data. Three different data sets from Pleiades and IKONOS are used for validation. The visual outcomes and quantitative measures approve the superiority of the proposed pan-sharpening method in balancing spatial enhancement and spectral preservance in the fused image. The proposed method also accomplishes optimal values for all the metrics at full-scale experimentation and RMSE, and CC at reduced-scale experimentation.

Author Contributions

A. Sharifi carried out the data analysis and interpreted the results and wrote the manuscript.

Acknowledgment

Thank you to Eng. Sadeghi Naeini to supply satellite data for this research.

Conflict of Interest

The author declares that there is no conflict of interests regarding the publication of this manuscript. In addition, the ethical issues, including plagiarism, informed consent, misconduct, data fabrication and/or falsification, double publication and/or submission, and redundancy have been completely observed by the authors.

Abbreviations

AWLP	Additive wavelet luminance proportional
ATWT	Atrous wavelet transform
CSR	Convolutional sparse representation
CC	Correlation coefficient
DWT	Discrete wavelet transforms
GS	Gram-Schmidt transform
HF	High frequency
LFC	Low-frequency component
HFC	High-frequency component
HRMS	High-resolution multispectral
IHS	Intensity-hue-saturation
LRMS	Low-resolution multispectral
MTF-GLP	Modulation transfer function-generalized lapalician pyramid
MS	Multi-spectral
PAN	Panchromatic
PS	Pan-sharpening
PCA	Principal component analysis
RMSE	Root mean square error
SR	Sparse representation
SAM	Spectral angle mapper
UIQI	Universal image quality index

References

[1] A. Kosari, A. Sharifi, A. Ahmadi, M. Khoshsima, "Remote sensing satellite's attitude control system: rapid performance sizing for passive scan imaging mode," Aircr. Eng. Aerosp. Technol., 92(7): 1073–1083, 2020.

[2] A. Sharifi, "Using Sentinel-2 Data to Predict Nitrogen Uptake in Maize Crop," IEEE J. Sel. Top. Appl. Earth Obs. Remote Sens., 13: 2656–2662, 2020.

[3] H. Demirel, G. Anbarjafari, "Discrete wavelet transform-based satellite image resolution enhancement," IEEE Trans. Geosci. Remote Sens., 49(6 PART 1): 1997–2004, 2011.

[4] H. Abdi, L. J. Williams, "Principal component analysis," Wiley Interdisciplinary Reviews: Computational Statistics, 2(4): 433–459, 2010.

[5] M. Oza, H. Vaghela, S. Bagul, "Semi-Supervised Image-To-Image Translation," in Proceeding - 2019 International Conference of Artificial Intelligence and Information Technology, ICAIIT 2019,: 16–20, 2019.

[6] A. Garzelli, B. Aiazzi, L. Alparone, S. Lolli, G. Vivone, "Multispectral pansharpening with radiative transfer-based detail-injection modeling for preserving changes in vegetation cover," Remote Sens., 10(8): 1–18, 2018.

[7] H. Loussifi, K. Nouri, N. Benhadj Braiek, "A new efficient hybrid intelligent method for nonlinear dynamical systems identification: The Wavelet Kernel Fuzzy Neural Network," Commun. Nonlinear Sci. Numer. Simul., 32: 10–30, 2016.

[8] S. Bama, D. Selvathi, "Despeckling of medical ultrasound kidney images in the curvelet domain using diffusion filtering and MAP estimation," Signal Processing, 103: 230–241, 2014.

[9] Y. Leung, J. Liu, and J. Zhang, "An improved adaptive intensity-hue-saturation method for the fusion of remote sensing images," IEEE Geosci. Remote Sens. Lett., 11(5): 985–989, 2014.

[10] G. Plonka, J. Ma, "Curvelet-wavelet regularized split Bregman iteration for compressed sensing," Int. J. Wavelets,

Multiresolution Inf. Process., 9(1): 79–110, 2011.

[11] L. Alparone, S. Baronti, B. Aiazzi, A. Garzelli, "Spatial Methods for Multispectral Pansharpening: Multiresolution Analysis Demystified," IEEE Trans. Geosci. Remote Sens., 54(5): 2563–2576, 2016.

[12] Z. Omar, T. Stathaki, "Image fusion: An overview," Proc. - Int. Conf. Intell. Syst. Model. Simulation, ISMS,: 306–310, 2015.

[13] Z. Shao, J. Cai, "Remote Sensing Image Fusion with Deep Convolutional Neural Network," IEEE J. Sel. Top. Appl. Earth Obs. Remote Sens., 11(5): 1656–1669, 2018.

[14] C. Jiang, Q. Zhang, R. Fan, Z. Hu, "Super-resolution CT Image Reconstruction Based on Dictionary Learning and Sparse Representation," Sci. Rep., 8(1), 2018.

[15] X. Yang, L. Jian, B. Yan, K. Liu, L. Zhang, Y. Liu, "A sparse representation based pansharpening method," Futur. Gener. Comput. Syst., 88: 385–399, 2018.

[16] B. Johnson, "Effects of pansharpening on vegetation indices," ISPRS Int. J. Geo-Information, 3(2): 507–522, 2014.

[17] S. Sulochana, R. Vidhya, K. Mohanraj, D. Vijayasekaran, "Effect of wavelet based image fusion techniques with principal component analysis (PCA) and singular value decomposition (SVD) in supervised classification," Indian J. Geo-Marine Sci., 46(2): 338–348, 2017.

[18] K. C. Jambu, S. D. Degadwala, D. Agrawal, "Satellite Image Fusion Using Adaptive Pan-sharpening Filters," 21(1): 16–19.

[19] J. Yang, J. Zhang, "Parallel performance of typical algorithms in remote sensing-based mapping on a multi-core computer," Photogramm. Eng. Remote Sensing, 81(5): 373–385, 2015.

[20] G. Masi, D. Cozzolino, L. Verdoliva, G. Scarpa, "Pansharpening by convolutional neural networks," Remote Sens., 8(7), 2016.

[21] B. Wohlberg, "Efficient algorithms for convolutional sparse representations," IEEE Trans. Image Process., 25(1): 301–315, 2016.

[22] Y. Liu, X. Chen, R. K. Ward, J. Wang, "Image Fusion with Convolutional Sparse Representation," IEEE Signal Process. Lett., 23(12): 1882–1886, 2016.

[23] J. Sulam, A. Aberdam, A. Beck, M. Elad, "On Multi-Layer Basis Pursuit, Efficient Algorithms and Convolutional Neural Networks," IEEE Trans. Pattern Anal. Mach. Intell.: 1–1, 2019.

[24] Y. Liu, S. Liu, Z. Wang, "A general framework for image fusion based on multi-scale transform and sparse representation," Inf. Fusion, 24: 147–164, 2015.

[25] S. Li, X. Kang, L. Fang, J. Hu, H. Yin, "Pixel-level image fusion: A survey of the state of the art," Inf. Fusion, 33: 100–112, 2017.

[26] A. Garzelli, "A Review of Image Fusion Algorithms Based on the Super-Resolution Paradigm," Remote Sens., 8(10): 1, 2016.

Biographies

Alireza Sharifi was born in Tehran, Iran, in 1981. He received a M.Sc. degree and a Ph.D. degree in Remote Sensing Engineering from the University of Tehran, Tehran, in 2008 and 2015, respectively. He is currently an Assistant Professor of Remote Sensing in the Faculty of Civil Engineering from the Shahid Rajaee Teacher Training University. In particular, he is involved in Earth Observation Programs, for the development of Precision Agriculture and also Environmental Monitoring with the help of satellite imagery.

How to cite this paper:

A. Sharifi, "Using Convolutional Sparse Representation and Discrete Wavelet Decomposition for Satellite Image Pan-sharpening," Journal of Electrical and Computer Engineering Innovations, 7(2): 205-212, 2019.

DOI: 10.22061/JECEI.2020.6297.296

URL: http://jecei.sru.ac.ir/article_1229.html